

The Difference between Flux Spectrums of WH-type Assembly and CANDU-type Lattice

Eun Hyun Ryu^{a*}, Yong Mann Song^a

^aKorea Atomic Energy Research Institute, 1045 Daedeok-daero, Yuseong-gu, Daejeon, 305-353, Korea

*Corresponding author: ryueh@kaeri.re.kr

1. Introduction

Because of the thermal peak of the microscopic fission cross section of the U-235 which will be loaded into the reactor core as a fuel material, the moderation process is very important in the neutron economy. It is natural that we can increase the fission rate by supplying neutrons with a suitable spectrum shape. Sometimes, the nuclear reactors are categorized by the material of the moderator because of its importance. The representative materials of the moderator are light water (H₂O) and heavy water (D₂O). Also, it is well known that the slowing-down ratio of D₂O is hundreds of times larger than that of H₂O while the slowing-down power of H₂O is several times larger than that of D₂O. This means that the H₂O sometimes plays a role of an absorber such as the liquid zone controller (LZC) in a CANDU-type reactor. It is thought that the flux spectrums in a different reactor can differ from each other. In this research, two representative assemblies (the Westinghouse (WH)-type fuel assembly of PWR and the CANDU-type fuel lattice of PHWR) are selected and the flux results for each group are extracted. Although there are many codes for the lattice transport calculation, the WIMS code and the HELIOS code are used for the calculation of the WH-type fuel lattice and the CANDU-type fuel lattice.

2. Problem Descriptions, Code Flows and Differences about Variable Setting

In this section the problem descriptions, code flows and differences regarding the variable setting are explained. Although the standard WH-type and CANDU-type lattice problems are famous, and thus there are not many details about these problems. In addition, the WIMS code and HELIOS package including AURORA, ZENITH, HOPE and PROLOG are also very famous. In this section, brief flows will be positioned. And in this research, the reference input for WH-type fuel is based on the technical report of KAERI [1]. It seems that the difference between the reference and input in this research is minor. However, to ensure that the accuracy of the result is retained, the differences between the two files are described.

2.1 Problem Descriptions

The power density of the WH-type fuel is 41.785W/gU and the boundary condition is reflective. The following are the pin cell geometry, dimensions,

and compositions. The enrichment and boron concentration are 4.3% at 500 ppm, respectively.

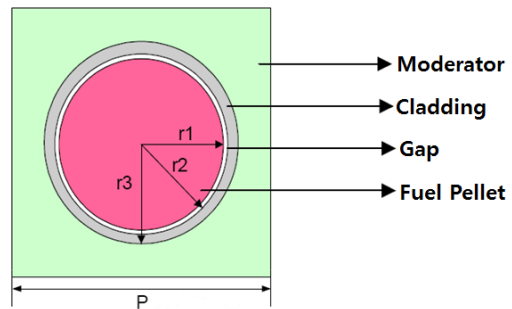


Fig. 1. Pin Cell Geometry of WH-type Lattice

Table I : Fuel and Gadolinium Pin Cell Parameters of WH-type Lattice

P	r1	r2	r3
1.2660	0.4096	0.4188	0.4759

Table II : Guide Tube Cell Parameters of WH-type Lattice

P	r1	r2	r3
1.2660	0.0	0.5624	0.6130

Table III : Material Composition WH-type Lattice

Material	Density (g/cm ³)	Nuclide	Weight(%)	Temperature (K)
Fuel	10.313	U	88.15	900
		O-16	11.85	
Air	0.001	O-16	100.00	636
Zry	6.55	Zr-2	100.0	636
Moo	0.659	H-1	11.19	600
		O-16	88.81	

There are two types of pin cells from a geometrical point of view, as shown in Tables I and II. Actually, however, we have three types of pin cell geometry, a fuel rod, a burnable poison rod (gadolinium rod) and a guide tube rod for device control. Among these three rod types, the dimensions of the fuel rod and burnable poison rod are same, as shown in Table I. The guide tube is empty because the variation regarding the control rod insertion is not considered in this research. The compositions of each material are provided in Table III. Because we are facing one reference case, the temperature variation is not considered either. In Table III, the 'Coo' material is not included because its composition is complicated. The material 'Coo' is for the coolant and thus it should include the grid (structural) material. The 'Moo' material is used for the inside of the guide tube.

Geometrically, 1/8 symmetry (octa core) is used. Thus, the pin cell is defined properly for its position in a

1/8 core, such as an octa cell, half cell, diagonally half cell, and full cell.

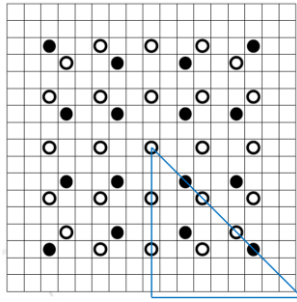


Fig. 2. Lattice of WH 16GD-type

In Fig. 2, the WH 16GD-type assembly is depicted and the actual calculation domain is also marked with a blue line. In the actual calculation domain, 3.125 guide tubes, 2 gadolinium rods, and 31 fuel rods are included.

The power density of the CANDU-type fuel is 33.4902W/gU and the boundary condition is reflective[2]. Because there is no pin cell in CANDU-type fuel, only the dimensions and compositions are included. The enrichment and the boron concentration in the moderator are 0.710971% and 2.5 ppm, respectively.

Table IV : Fuel Pin Cell Parameters of CANDU-type Lattice

P	r1	r2	r3
N/A	0.429709	0.607700	0.648080

Table V : Material Specifications of CANDU-type Lattice

Material	Density (g/cm ³)	Temperature(K)	Specification
Fuel	10.365	960.16	UO ₂
Cladding	6.520	561.16	Zr-4
Coolant	0.807859	561.16	D ₂ O purity 99.1 WT%
PT	6.515	561.16	Zr-Nb
Gap	0.00118	451.66	CO ₂
CT	6.544	342.16	Zr-2
Moder	1.085089	342.16	D ₂ O purity 99.85 WT%

Because there is no pin cell geometry in the lattice of the CANDU-type, the pitch of the cell is not defined. Also, in the WIMS code, the gap between the fuel pellet and cladding is not defined and thus the gap region is filled with the fuel material.

The following are the description of the lattice of CANDU-type and lattice dimensions.

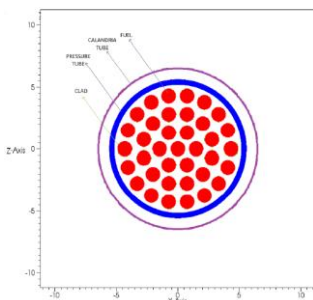


Fig. 3. Lattice of CANDU-type

Table VI. Dimensions of Lattice of CANDU-type

Lattice Pitch	Fuel Bundle length	Inner Radius of Pressure Tube
28.575	49.53	5.17915
Outer Radius of Pressure Tube	Inner Radius of Calandria Tube	Outer Radius of Calandria Tube
5.61266	6.44988	6.58954

Table VII. Array Dimensions of Lattice of CANDU-type

Pitch Circle Radius of Inner Ring	Pitch Circle Radius of Middle Ring	Pitch Circle Radius of Outer Ring
1.488450	2.875300	4.330700
Angular Offset of Inner Ring	Angular Offset of Middle Ring	Angular Offset of Outer Ring
0	2.61799radians	0

In Fig. 3., the large volume of the lattice cell in a CANDU-type lattice is occupied with the moderator while the relative small volume of the lattice cell is occupied in the WH 16GD-type lattice. In Table VI, it can be verified that the lattice pitch of the CANDU-type is larger than that of WH 16GD-type.

2.2 Code Flows

The flux spectrum result for PHWR lattice is obtainable by using only the WIMS code[3], and thus there are not much things to explain about code flow. The important options are FEWGROUPTS and SUPPRESS. The FEW GROUPS command is for the specification of the energy bounds, which is the number of cross section libraries that will be provided with the WIMS code. Usually, 4, 8, 12, 16, 20, 22, 24, 26, 28, 31, 35, 39, 41, 44, 47, 50, 53, 56, 59, 62, 65, 67, 69, 71, 73, 75, 77, 79, 81, 83, 85, 87 and 89th energy bounds are used for the 33 group calculation. In addition, the FEWGROUPTS command is not only for the input specification but also for the output specification. The SUPPRESS command is for the output control. If the 'regional and cell edit' option in SUPPRESS is used, then the cell and region-wise averaged and integrated fluxes for groups are obtainable.

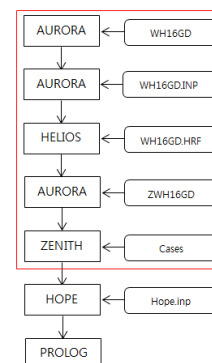


Fig. 4. Overall Code Flow

In Fig. 4, the main input file is specified and the code flows that were used in this research are marked with a red line. Because of the readability and maintenance, the main input file is split into two files, 'WH16GD' and

‘WH16GD.INP’. Practically, the code flows of AURORA, HELIOS and ZENITH are of multi-dimensions because of the multiple communications between codes used in this research and hermes files such as ‘WH16GD.hrf’, ‘WH16GD.out’ and library file ‘hy190n48g17a.dat’ [4],[5],[6],[7].

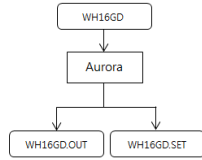


Fig. 5. AURORA Code Running1

In Fig. 5, the ‘WH16GD’ file contains CCS structures and many variables such as temperatures, pressure, density and material composition assignments.

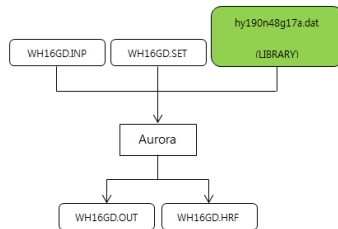


Fig. 6. AURORA Code Running2

In Fig. 6, the ‘WH16GD.INP’ file contains information regarding the assembly connectivity, material assignment, path definition, and boundary condition.

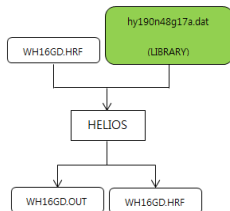


Fig. 7. HELIOS Code Running

With the interpretation of the AURORA code about the input files, the HELIOS code is now ready to run with the produced hermes file, ‘WH16GD.HRF’, as in Fig. 7. The number of neutron energy groups, gamma energy group, and version and status of the library are 190, 48, and 1.7 and adjusted, respectively.

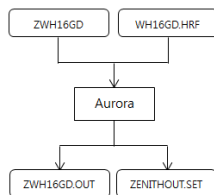


Fig. 8. AURORA Code Running3

In Fig. 8., file ‘ZWH16GD’ file includes the definition of variables related with the interested parameter that will be printed in the output files of the

ZENITH code. The ‘ZWH16GD.OUT’ file shows the running result of the AURORA code, and the ‘ZENITHOUT.SET’ file is a binary file that will be provided with the ZENITH code.

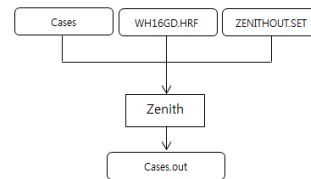


Fig. 9. ZENITH Code Running

Originally, all results about the input files for the current problem are included in the ‘WH16GD.HRF’ file. However, to see and retrieve the necessary parameter, the ZENITH code should be used. And in this stage, the branch calculation is conducted. As in Fig. 9, case files and a pre-generated zenith input file ‘ZENITHOUT.SET’ are necessary in addition to the ‘WH16GD.HRF’ file.

2.3 Differences about Variable Setting

Although any number of groups is possible within the ENDF-VI library, the energy bounds of 33 groups are chosen for both simulations of lattices of PWR and PHWR. Although the energy bound of 33 groups from ENDF-VI library is specified in the AURORA input, the HELIOS determines the energy bound as the nearest one among the energy bounds within its own library from a user-specified value. Because the options for number of groups of the HELIOS library are limited to 190, 112, and 47 and the energy bound is not consistent with the ENDF-VI library, the library of 190 energy groups is chosen for operating HELIOS because of ambiguous points in the operation [6].

The coupling option of the assemblies is 2 for this research which is different from reference [1]. For the cladding material, isotope 40002 is used instead of 40010, which is the isotope for the cladding material in reference [1]. For computational convenience, the number of node divisions for the pin cell area, with the exception of the CCS region, is reduced to 4 instead of 8, which is the number of node divisions in reference [1]. Although it is good to refine the CCS region (especially for the burnable poison rod, i.e. gadolinium rod), the number of divisions for the pin geometry is reduced, i.e., 4 for the fuel pin, 12 for the gadolinium pin, and there is no change in the control rod (6) [1]. In addition, the 12 additional paths including fuel, and moderator temperature variations are added. However, in this paper, only the reference case is analyzed. Finally, 147.959 bar (146.024 ATM) is used for the system pressure with the given data in the reference (from a steam table with coolant conditions with a density of 0.659g/cm at 600K) [1]. Finally, the boron concentration of the CANDU-type fuel in reference is

2.5ppm in the moderator [2]. However, in this research, the boron concentration is set to zero.

3. Results

The result of WIMS code is compared with that of the McCARD code for confirmation of the soundness of the input for the CANDU-type lattice. The following are comparisons of the flux spectrum and the thermal and fast flux portions for each code with a zero boron concentration.

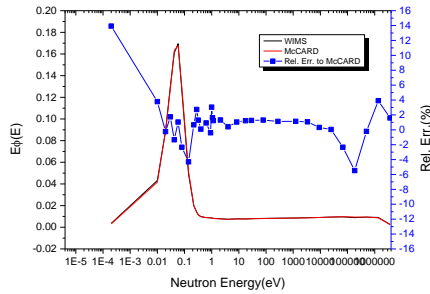


Fig. 10. Flux Spectrum Comparison between Results of WIMS and McCARD Codes

In Fig. 10, it can be confirmed that the spectrum of WIMS Code is well matched with that of the McCARD code(using infinite spectrum)[8]. The portion of fast flux and thermal flux($E\phi(E)$) is almost the same as each other for 17% and 83%.

Although the main aim of this research is to investigate the difference between spectrums of the PWR and PHWR, the spectrum changes with boron concentration are also included to see the thermal neutron change about the WH 16GD-type. Two cases of boron concentrations of 0ppm and 500ppm are simulated. All tables for the portion of the fast and thermal flux has bound of 0.625eV.

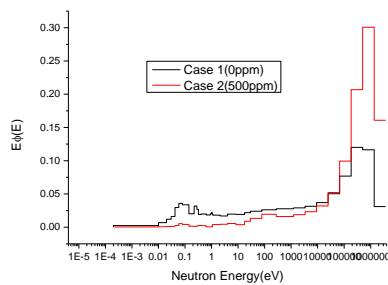


Fig. 11. Spectrum Change with Boron Concentration for WH 16GD-type

Table VII. Fast and Thermal Flux Portion for WH 16GD-type (bound of 0.625eV)

	Case 1	Case 2
Fast(%)	76.52	97.71
Thermal(%)	23.48	2.29

In Fig. 11 and Table VII., it can be recognized that the effect of boron is to reduce the thermal flux because of the microscopic absorption cross section of the boron is decreasing with the incident neutron energy at the log scale. The extreme influence of the boron can be verified in the Fig. 11 and Table VII.

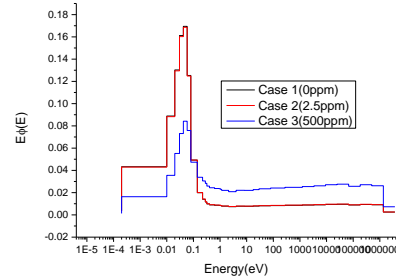


Fig. 12. Spectrum Change with Boron Concentration for CANDU-type

Table VIII. Fast and Thermal Flux Portion for CANDU-type

	Case 1	Case 2	Case 3
Fast(%)	17.36	17.67	49.26
Thermal(%)	82.64	82.33	50.74

As we can see in Fig. 12 and Table VIII, in contrast with the case of PWR, the effect of the boron of the PHWR is much larger than that of the PWR because of the much more thermalized spectrum due to the heavy water.

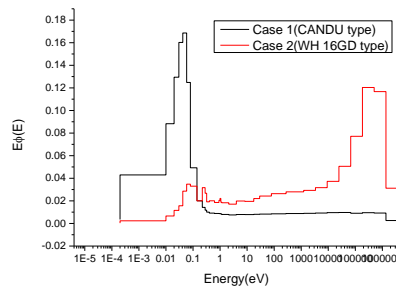


Fig. 13. Flux Spectrum Comparison between Results of WH 16GD-type and CANDU-type.

Table IX. Fast and Thermal Flux Portion for Codes

	Case 1	Case 2
Fast(%)	17.67	76.97
Thermal(%)	82.33	23.03

In Fig. 13 and Table IX, the difference between spectrums of PWR and PHWR can be well verified through the WH 16GD-type and CANDU-type lattices. In spite of the zero boron in the WH 16GD-type, the portion of the thermal flux in CANDU is about four times more higher than that in PWR as 82.33%.

4. Conclusions

In this research, the investigation about flux spectrums in PWR and PHWR is done through the representative problems of WH 16GD-type and CANDU-type lattices. A clear difference in spectrum between the CANDU-type lattice and WH 16GD-type lattice is confirmed. Because of the superior moderating ratio of the heavy water, the thermal flux ratio of the CANDU-type lattice is almost 82%, while that of the WH 16 GD-type lattice is around 23%.

Because of the large portion of the thermal flux in the CANDU-type lattice, the boron effect is maximized with the result from variations of boron. Thus it can be said that the spectrum largely depends on the moderator material, and the boron effect and sensitivity largely depends on the flux spectrum.

Because of the dominant effect of the moderator material on the flux spectrum in a nuclear reactor, in the future, a comparison of the spectra of SFR, HTGR, PWR, and PHWR are also an interesting subject to study. In addition, it seems that utilizing the McCARD code can give us more accurate results with refined group spectrums about result and simplicity regarding the core inputs because of using one code.

Also, over-moderation in PHWR lattice and under-moderation in PWR lattice can be explained by the investigation about flux spectrums with variations of moderator density in each lattice.

5. Acknowledgement

This work was supported by the National Research Foundation of Korea(NRF) grant funded by the Korea overnment(Ministry of Science, ICT, and Future Planning) (No. NRF-2012M2A8A4025966)

REFERENCES

- [1] Hyung Jin Shim et al., Evaluation of CASMO-3 and HELIOS for Fuel Assembly Analysis from Monte Carlo Code, KAERI/TR-3417/2007, Korea Atomic Energy Research Institute, 2007.
- [2] KHNP, Design Manual, CANDU 6 Generating Station, Physics Design Manual, Wolsong NPP 1, 59RF-03310-DM-000 Revision 0, 2001.
- [3] S.R. Douglas, WIMS-AECL Release 2-5d User's Manual, COG-94-52(Rev. 4), FFC-RRP-299, AECL, Jul., 2000.
- [4] AURORA User Manual, Studvik, Ver. 1.9, 2005.
- [5] ZENITH User Manual, Studvik, Ver. 1.9, 2005.
- [6] HELIOS Methods, Studvik, Ver. 1.9, 2005.
- [7] HELIOS Program, Studvik, Ver. 1.9, 2005.
- [8] Hyung Jin Shim and Chang Hyo Kim, McCARD User's Manual, Ver. 1.1, 2013.